Causal Evidence for the Role of Neuronal Oscillations in Top–Down and Bottom–Up Attention

Justin Riddle, Kai Hwang, Dillan Cellier, Sofia Dhanani, and Mark D'Esposito

Abstract

■ Beta and gamma frequency neuronal oscillations have been implicated in top–down and bottom–up attention. In this study, we used rhythmic TMS to modulate ongoing beta and gamma frequency neuronal oscillations in frontal and parietal cortex while human participants performed a visual search task that manipulates bottom–up and top–down attention (single feature and conjunction search). Both task conditions will engage bottom–up attention processes, although the conjunction search condition will require more top–down attention. Gamma frequency TMS to superior precentral sulcus (sPCS) slowed saccadic RTs during both task conditions and induced a response bias to the contralateral visual field. In contrary, beta frequency TMS to sPCS and intraparietal sulcus decreased search accuracy only during the conjunction search condition that engaged more top–down attention. Furthermore, beta frequency TMS increased trial errors specifically when the target was in the ipsilateral visual field for the conjunction search condition. These results indicate that beta frequency TMS to sPCS and intraparietal sulcus disrupted top–down attention, whereas gamma frequency TMS to sPCS disrupted bottom–up, stimulus-driven attention processes. These findings provide causal evidence suggesting that beta and gamma oscillations have distinct functional roles for cognition. ■

INTRODUCTION

Neuronal oscillations are proposed to be a fundamental mechanism that supports a diverse range of neural processes (Fries, 2015; Canolty & Knight, 2010), and oscillations at different frequency bands could contribute to distinct cognitive processes (Siegel, Donner, & Engel, 2012). For example, neurophysiology recordings in monkeys demonstrated that directed coherence of beta frequency oscillations from frontal to parietal cortex mediated top–down attention during a conjunction feature search task (Buschman & Miller, 2007), whereas directed coherence of gamma oscillations from parietal to frontal cortex mediated bottom–up, stimulus-driven attention in a single-feature search task. Other monkey and human studies have also found that gamma frequency oscillations carry sensory feed-forward information across the cerebral cortex, whereas feedback modulatory information is carried in the beta frequency (Michalareas et al., 2016; Bastos et al., 2015). Given that neurophysiology recordings can only provide correlational evidence, a causal manipulation is required to provide evidence that neuronal oscillations are not an epiphenomenon of the underlying neuronal computation (Fröhlich & McCormick, 2010; Buzsáki, 2006).

Rhythmic TMS has been demonstrated to entrain neuronal oscillations in human EEG data (Albouy, Weiss, Baillet, & Zatorre, 2017; Hanslmayr, Matuschek, & Fellner, 2014; Thut et al., 2011), making it a powerful approach to causally manipulate and dissociate the specific roles of neuronal oscillations in different frequency bands (Quentin et al., 2016; Chanes, Quentin, Tallon-Baudry, & Valero-Cabré, 2013; Romei, Driver, Schyns, & Thut, 2011; Romei, Gross, & Thut, 2010). Here, we used rhythmic TMS to modulate ongoing neuronal oscillations in the beta (20 Hz) and gamma (50 Hz) frequency while human participants performed a visual search task. The task, adopted from the Buschman and Miller (2007) study, manipulates levels of top–down attention while participants search for a visual target. When visual search requires evaluation of a conjunction of two or more stimulus features, top–down serial attention is required (Treisman & Gelade, 1980), whereas single-feature search only requires parallel and automatic bottom–up attention (Nakayama & Silverman, 1986). fMRI studies that have contrasted conjunction versus feature search found activation in the superior precentral sulcus (sPCS) and intraparietal sulcus (IPS; Donner et al., 2002). These regions have long been implicated in visual attention (Corbetta & Shulman, 2002) and are the same regions where neuronal recordings were taken in the Buschman and Miller (2007) study. Therefore, in our human fMRI study, we applied beta and gamma frequency TMS to the sPCS and IPS during the performance of the visual search task.

On the basis of previous studies that showed involvement of gamma frequency oscillations in bottom–up,

University of California, Berkeley

feed-forward, stimulus-driven attention processes (Kornblith, Buschman, & Miller, 2016; Marshall, O'Shea, Jensen, & Bergmann, 2015; Gregoriou, Gotts, Zhou, & Desimone, 2009; Börgers & Kopell, 2007), we hypothesized that gamma frequency TMS would modulate performance during both the feature and conjunction search conditions because both conditions required bottom–up attention to process visual stimuli. In contrast, on the basis of the involvement of beta frequency oscillations in top–down attention selection (Antzoulatos & Miller, 2016; Stanley, Roy, Aoi, Kopell, & Miller, 2016; Stoll et al., 2016; Buschman & Miller, 2009), we hypothesized that beta frequency TMS would modulate performance only during the conjunction search condition that engaged more top–down attention. One previous study has found that gamma-band activity in IPS influenced gamma-band activity in sPCS during bottom–up attention, whereas beta-band activity in sPCS influenced beta-band activity in IPS (Buschman & Miller, 2007) during top–down attention. This result suggests that there will be a potential interaction between the brain region that we target with TMS and the TMS frequency. Rhythmic TMS may directly modulate neuronal oscillations in the targeted region that transmits oscillatory signals to other connected regions and thus may impact behavior. According to this model, gamma TMS should have a greater impact on behavior when applied to IPS during bottom–up attention, and beta TMS would have a greater impact on behavior when applied to sPCS during top–down attention. Alternatively, rhythmic TMS may modulate the state of a region receiving oscillatory signals from other regions, thus modulating its receptivity to neuronal activity that is timed to the frequency of TMS. If this is the case, gamma TMS to sPCS will have an impact on behavior during bottom–up attention, and beta TMS to IPS will impact behavior during top–down attention.

METHODS

After obtaining informed consent according to the guidelines of the Committee for the Protection of Human Subjects at the University of California, Berkeley, 17 participants (nine women, ages 18–38 years, $M = 21.3$, $SD = 4.5$) participated in one session of fMRI and three sessions of online rhythmic TMS. Eight additional volunteers completed the MRI session but were subsequently dropped from the study because of excessive head motion ($n = 3$) or inability to meet the time commitment of the study ($n = 5$). We further excluded one male participant's data because his behavioral performance was 3 *SD*s away from the group average, leaving 16 participants in the reported results.

Visual Search Task

The behavioral task used in all four sessions of our experiment was adapted from a previous study (Buschman & Miller, 2007) consisting of three epochs (Figure 1A). In the first epoch, a sample stimulus was presented for 1 sec and had two features: color (red, green, or blue) and orientation (60°, 105°, or 150°). The width of the sample stimulus was 1 visual degree during fMRI scanning and 2.5° after TMS administration. In the second epoch, the screen went black for a short delay period of 500 msec. Participants were instructed to maintain fixation for the duration of the sample and delay epochs. Finally, during the response window epoch, a probe of four stimuli appeared at the corners of the screen (2.5° from fixation during fMRI, 7° during TMS). Stimuli were presented in the visual periphery to maximize discrimination of the saccade direction. The sample stimulus was always one of the four probe stimuli. Participants were instructed to perform a saccade and fixate on the probe

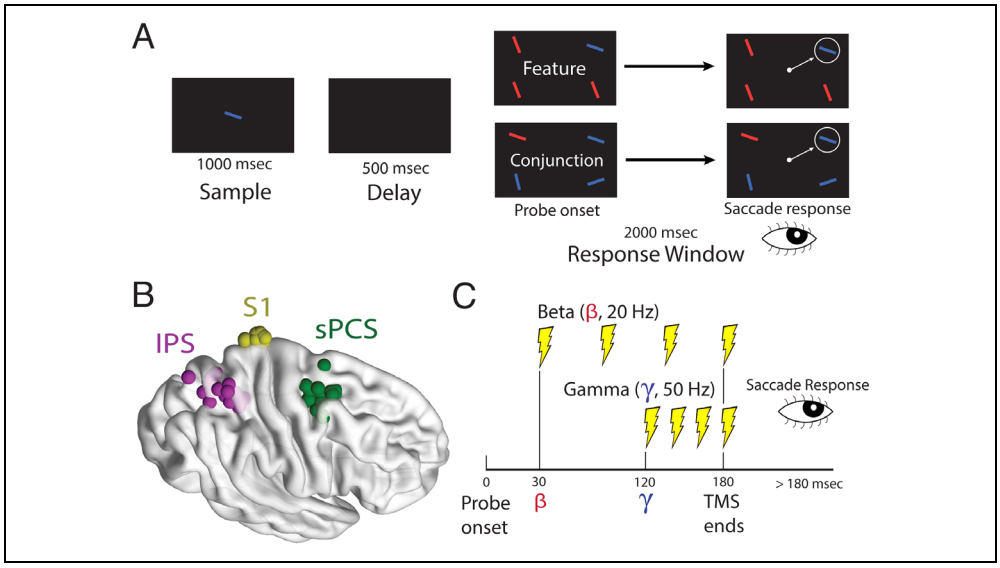

Figure 1. Experimental design. (A) The two conditions of the visual search task. (B) Participant-specific ROIs localized by fMRI data and targeted by TMS. (C) Timing of rhythmic TMS during each trial.

stimulus that was identical to the sample stimulus, to be fast and accurate, and to respond within the 2-sec response window in which the probe was present. The key manipulation in this task was the similarity between the sample stimulus and the three distractor stimuli in the probe. In the feature task, the three distracting stimuli were uniform and did not share a common feature with the sample stimulus. In this task, the salient difference between the sample stimuli and the distractors was sufficient to allow participants to successfully perform the task through bottom–up, stimulus-driven attention and minimal top–down attention (Fries, 2015; Börgers & Kopell, 2007; Nakayama & Silverman, 1986; Treisman & Gelade, 1980). In the conjunction search task, each distracting stimulus was unique and matched the sample stimulus in either color or orientation. The participant had to withhold a response and perform a serial search of the array for the stimuli that matched the sample stimulus in both features. In addition to bottom–up attention, this task required more top–down attention than the feature task (Buschman & Miller, 2009; Nakayama & Silverman, 1986; Treisman & Gelade, 1980). In neither task was a fixation cross present during the delay and response probe epochs because previous research has shown that, without the central fixation, the oculomotor system has a lower threshold for generating saccades in reaction to sensory inputs (Reuter-Lorenz, Hughes, & Fendrich, 1991). In this way, we were able to increase our sensitivity of detecting TMS effects on search accuracy.

Between trials, participants fixated on a centrally presented cross. During the fMRI session, the intertrial interval was selected from an exponential distribution between 3 and 10 sec to maximize statistical power in the fMRI analysis (Dale, 1999). During the TMS sessions, the intertrial interval was randomly selected to be either 2, 4, or 6 sec.

Stimuli were presented using a custom script in MATLAB (The MathWorks, Inc.) with the Psychophysics Toolbox extensions Version 3. During the fMRI session, the screen resolution was 800 × 600 and back-projected by an AVOTEC projector with a 60-Hz refresh rate onto a 20 × 15 cm screen that was 120 cm from the eye. During the three TMS sessions, stimuli were presented on a 34 × 27 cm LCD monitor presented 74 cm from the eye with 1280 × 1024 resolution and a 60-Hz refresh rate.

Participant responses were measured using eye trackers. During the fMRI session, the participant's eye position was recorded by an Eyelink 1000 Plus Long-Range Mount (SR Research; Version 5.0.4 software) that was calibrated before the first run. During TMS sessions, an Eyelink 1000 Plus Desktop Mount with Version 5.0.4 software was used to collect saccade data that was calibrated at the start of each block of six runs. Participants were instructed to press their head to a forehead mount for consistent eye tracking.

A custom MATLAB script was used for analysis that utilized Eyelink's automated software for saccade detection during acquisition. Participants were instructed to saccade and fixate on the sample item within the array of probe stimuli and to be "fast and accurate." Each trial was scored for saccadic RT (the time when a saccade was initiated toward a peripheral target) and search accuracy (correct was defined as a single saccade to the target). Participants could have had a correct target selection in a trial as indicated by their final fixation but overtly performed saccades to multiple distractor stimuli before selecting the correct target, therefore rendering the search accuracy incorrect. Given that gaze may drift without a fixation cross, trials in which the gaze drifted 3° visual angle in TMS (1° visual angle in fMRI) from the center of the screen before presentation of the probe were removed from analysis. On average, only 2% of trials with a standard deviation of 1% across participants were removed because of gaze drift. After the automated eye tracker analysis script was run, experimenters manually checked each trial and corrected any mistakes or failures of the automated analysis.

MRI Protocol

During the first session of the experiment, MRI data were collected on a Siemens 3-T MAGNETOM Trio using a 12-channel receive-only coil at the Henry H. Wheeler, Jr. Brain Imaging Center at the University of California, Berkeley. First, an anatomical image was collected using a T1-weighted magnetization prepared rapid gradient echo sequence with 192 sagittal slices each, 1-mm isotropic voxels, 50% distance between slices (0.5 mm), 2.3-sec repetition time, interleaved slice acquisition, phase-encoding direction from anterior to posterior, 2.98-msec echo time, 9° flip angle, and parallel imaging via Generalized Autocalibrating Partial Parallel Acquisition with an acceleration factor of 2. Next, functional data were collected during performance of the visual search task using a T2*-weighted single-shot EPI sequence with 37 slices each, 3.5-mm isotropic voxels, 20% distance between slices (0.7 mm), 2-sec repetition time, descending slice acquisition, phase encoding direction anterior to posterior, 24-msec echo time, 60° flip angle, fat saturation, and prescan normalization. The first two volumes of every functional run were discarded upon acquisition, and for analysis purposes, the first two recorded volumes were also discarded.

Preprocessing of fMRI data was performed using the Statistical Parametric Mapping 12 toolbox (SPM12, www.fil.ion.ucl.ac.uk/spm) in MATLAB (Version 2014a release). All preprocessing steps were performed in SPM12, unless otherwise noted. The anatomical image had the neck removed (AFNI; Cox, 1996), manual reorientation to the anterior commissure, segmentation with mean bias correction, and skull stripping (FSL 4.1.9, fsl.fmrib.ox.ac.uk/fsl/). The functional data were de-spiked at 3 *SD*s above the mean (AFNI), slice time corrected, rigid body motion aligned to the mean functional image, manually reoriented to the anterior commissure, and smoothed with an FWHM kernel of 4 mm.

ROI Localization

After the first session, a univariate analysis of the fMRI data was performed in each participant's native space with a general linear model analysis that included eight nuisance regressors: six rigid body motion realignment parameters and the mean signal in white matter and cerebrospinal fluid. The masks for white matter and cerebrospinal fluid were calculated by SPM12's segmentation of the anatomical image. Each trial was modeled as an event with onset at the start of the sample epoch and duration until the end of the saccade response. If no saccade was made, then the event duration included the full 2-sec response window. The onset and duration of these events were convolved with the canonical hemodynamic response function, and five task regressors were generated: correct and incorrect feature and conjunction search, and miss trials.

The activation map for all correct trials was used to identify ROIs for targeting with TMS in Sessions 2, 3, and 4. The participant-specific ROIs were normalized into the Montreal Neurological Institute's (MNI) standardized space for display purposes (Figure 1B). A previous study that applied TMS to both left and right sPCS during a visual search task found that only TMS to the right hemisphere modulated behavior (Muggleton, Juan, Cowey, & Walsh, 2003). Thus, to maximize the effect of beta versus gamma frequency TMS, we chose to stimulate the right hemisphere and hypothesized that behavioral changes would be restricted to the left visual field.

The right sPCS ROI was defined as the peak contrast value at the intersection of the precentral sulcus and superior frontal sulcus. The coordinates of the average sPCS ROI in MNI space after normalization was $x = 27$ mm, $y = 0$ mm, and $z = 57$ mm, with standard deviations of $x = 5$ mm, $y = 5$ mm, and $z = 6$ mm. Averaged across participants, the sPCS ROI was 28.5 mm from the scalp with a standard deviation of 5.4 mm. sPCS is the human analog of the FEFs typically defined as the region at which electrical stimulation of neurons resulted in contralateral eye movements (Robinson & Fuchs, 1969). sPCS has contralateral visual field maps and plays a prominent role in saccadic eye movements to the periphery but may play a more extensive role in humans from its involvement in attention and cognitive control (Vernet, Quentin, Chanes, Mitsumasu, & Valero-Cabré, 2014).

The right superior IPS ROI was defined as the peak activation in the dorsal region of the IPS. The coordinates of the average IPS ROI in MNI space after normalization was $x = 29$ mm, $y = -56$ mm, and $z = 56$ mm with standard deviations of $x = 7$ mm, $y = 9$ mm, and $z = 6$ mm. Averaged across participants, the IPS ROI was 27.9 mm from the scalp with a standard deviation of 7.3 mm. Previous fMRI studies of visual search have found this superior IPS region to be involved in conjunctive feature search greater than single-feature search (Shulman et al., 2003; Donner et al., 2002). The homologous region in monkeys, the lateral intraparietal area, is considered most equivalent in anatomy and function to the IPS ROI targeted in this experiment (Grefkes & Fink, 2005).

The right primary sensory cortex (S1) ROI was defined as the dorsal medial region of the post central gyrus and roughly corresponds to sensory input from the legs. No significant task-related modulation was found in the S1 ROI during fMRI across participants. The coordinates of the average S1 ROI in MNI space were $x = 8$ mm, $y = -39$ mm, and $z = 79$ mm with standard deviations of $x = 1$ mm, $y = 3$ mm, and $z = 2$ mm. Averaged across participants, the S1 ROI was 22.5 mm from the scalp with a standard deviation of 2.7 mm. S1 was used as a control stimulation site to account for nonspecific TMS effects. This site has been demonstrated to be an effective control site for TMS stimulation of the oculomotor network given its close proximity to the oculomotor network and its inactivity during saccadic tasks (Cameron, Riddle, & D'Esposito, 2015). The average distances between TMS target sites were as follows: sPCS and IPS, 57 mm; IPS and S1, 38 mm; and sPCS and S1, 49 mm. The spatial resolution of TMS has been demonstrated as sufficient to dissociate ROIs with this distance (Wagner, Rushmore, Eden, & Valero-Cabré, 2009).

The distance from scalp to cortical ROI systematically alters the effectiveness of TMS (Stokes et al., 2005). However, in this study, the scalp to cortex distance was not different between sPCS and IPS, $t(15) = 0.32$, $p = .75$, $d = 0.08$, suggesting that rhythmic TMS should be similarly effective to both TMS targets. The S1 control site was significantly closer to the scalp than both sPCS, $t(15) = 5.68$, $p = .00004$, $d = 1.42$, and IPS, $t(15) = 3.2$, $p = .005$, $d = 0.81$. Thus, any difference in TMS effect between the control site and either the sPCS or IPS cannot be explained by reduced efficacy of TMS to modulate the S1 control site.

TMS

During Sessions 2, 3, and 4 of the experiment, TMS was delivered using a MagStim Super Rapid-2 Plus1 stimulator with a figure-of-eight 70-mm double air film coil. Each participant's motor threshold (MT) was calculated to calibrate the coil intensity to their specific sensitivity level. To calculate a participant's MT, an electrode was attached to the first dorsal interosseous muscle on the left hand of the participant. Single pulses of TMS were delivered to the corresponding hand region of the motor cortex at a 45° angle until the TMS pulses reliably elicited a motor evoked potential (MEP), defined as a near-instantaneous voltage increase of at least 70 μV above baseline (O'Shea, Johansen-Berg, Trief, Göbel, & Rushworth, 2007). Once an MEP was generated, the intensity was decreased to a level that elicited an MEP on 5 of 10 pulses.

To trigger the TMS coil during online TMS, a custom-built serial cable triggered trains of four biphasic pulses

with an interpulse interval of either 20 Hz (beta frequency) or 50 Hz (gamma frequency) at high or low (110% or 50% of MT) coil output. The low-intensity TMS was beneath the threshold for modulating neuronal activity; therefore, we hypothesized that high-intensity TMS would result in stronger behavioral modulation compared with low-intensity TMS. During online TMS, participants were actively monitored for signs of duress and were encouraged to inform the experimenter of any discomfort. For one participant, TMS to sPCS elicited muscle twitching and the TMS amplitude was lowered by 5% to reduce head movement.

To ensure the accuracy of TMS targeting, we used Rogue Research's BrainSight v2.2.11 with a Northern Digital Polaris Spectra infrared camera to register coordinates around the participants' head to their anatomical MRI scans with stereotaxic 3-D tracking. Participant-specific ROIs derived from the fMRI data were overlaid on the participant's anatomical image, and a trajectory for TMS was calculated to be perpendicular to the skull. The coil angle was held constant in the posterior to anterior direction for all three ROIs. During the TMS sessions, experimenters actively maintained a stable position of the TMS coil aided by a MagStim coil holder and continuous stereotaxic tracking. We maintained the TMS coil position to be under 5 mm and 5 degrees of error.

A previous monkey primate electrophysiology study with a similar visual search task demonstrated that, upon presentation of the probe, the identity of the target stimulus could be decoded from spiking activity in frontal and parietal cortex (Buschman & Miller, 2007). Beta and gamma oscillations were observed in the 200 msec after the probe onset before the monkey made a saccade (Buschman & Miller, 2007). On the basis of these findings, in our study, rhythmic TMS was delivered such that the four-pulse train ended at 180 msec after the presentation of the probe (Figure 1C). Crucially, the timing of rhythmic TMS was chosen to maximally align frequency-specific stimulation to coincide with the coherence effect previously reported. Thus, beta frequency TMS started 30 msec after the onset of the probe, and gamma frequency started 120 msec after the onset of the probe.

During each session of online rhythmic TMS, participants completed one block of beta frequency TMS at 20 Hz and one block of gamma frequency TMS at 50 Hz in counterbalanced order across participants. Participants were given a minimum of a 10-min break between the two blocks. Each block consisted of six runs of 32 trials each with a short self-paced break between each run. Within each run, there were two task conditions (feature or conjunction search) and two TMS intensity conditions (110% or 50% of MT), which were randomized and counterbalanced. Overall, participants completed 384 trials on each TMS day with 48 trials in each experimental condition. After removal of trials in which the participant broke fixation or performed a saccade before the completion of TMS, the average number of trials per condition was 34.5 (median = 38.9) with a standard deviation of 10.4.

Statistical Analysis

The frequency-specific effects of TMS on participant performance were assessed based on saccadic RT for correct trials and search accuracy. We hypothesized that TMS would have a frequency-specific impact on performance. Gamma frequency TMS should impact behavioral performance during both the feature and conjunction search tasks (both employed bottom–up attention), while beta frequency TMS should impact behavioral performance only during the conjunction search task (greater top–down attention was required). On the basis of this prediction, we performed two repeated-measures ANOVA using RT and Search accuracy as dependent variables and Task condition (feature vs. conjunction search), TMS frequency (beta vs. gamma), and TMS site (sPCS and IPS) as independent variables. Given our focus on beta and gamma frequency oscillations, we tested for a main effect of TMS frequency or an interaction of frequency with other experimental factors. After identifying significant main or interaction effects, we performed follow-up post hoc t tests while controlling for multiple comparisons using Tukey's correction procedure.

To control for nonspecific physiologic effects of rhythmic TMS such as auditory entrainment and the general effect of noninvasive brain stimulation to the brain, all analyses are reported as the difference in performance after TMS to sPCS or IPS compared with condition-matched TMS to the S1 control site. We expected that low-intensity TMS would have a reduced, or negligible, impact on behavioral performance because it was delivered below the MT. Therefore, we also performed two control ANOVAs on the low-intensity TMS conditions.

Receptive fields in sPCS and IPS are lateralized to represent the contralateral visual field (Silver & Kastner, 2009), and previous research found that gamma frequency TMS to sPCS resulted in an increase in reporting the detection of a low contrast stimulus in the contralateral visual field even when the stimulus was not present, essentially creating a phantom bottom–up signal (Chanes et al., 2013). Therefore, gamma frequency TMS to sPCS could systematically bias participants to saccade to the contralateral visual field as bottom–up attention is engaged. Given that TMS was applied to the right hemisphere, we calculated response bias as the number of error trials with the first saccade toward the left visual field divided by the total number of error trials. Note that the probability of stimuli presented in each visual field was 50%.

Previous research on beta frequency rhythmic TMS to sPCS found an increase in d', a metric of successful signal

detection, in the contralateral visual field (Chanes et al., 2013). Thus, we hypothesized that beta frequency TMS would modulate top–down attention signals toward the contralateral visual field resulting in a search bias. We calculated search bias as the number of error trials with the target in the ipsilateral visual field divided by the total number of error trials. For example, a search bias toward the contralateral visual field reflects reduced saccade accuracy when the target was in the ipsilateral visual field.

RESULTS

Our experiment was designed to test for frequency-specific effects of beta versus gamma frequency TMS on saccadic RT and search accuracy of a visual search task. We predicted an effect of high-intensity gamma frequency TMS on both feature and conjunction search conditions given that both conditions employed bottom–up attention. We also predicted an interaction of high-intensity beta frequency TMS and task condition given that the conjunction search condition likely engaged more top–down attention. Given that receptive fields in sPCS and IPS are lateralized to represent the contralateral visual field (Silver & Kastner, 2009), we predicted that high-intensity gamma frequency TMS would lead to a contralateral response bias and high-intensity beta frequency TMS would lead to a contralateral search bias.

Task Effects: Saccadic RT

We first performed a three-way (Task Condition × TMS Frequency × TMS Site) repeated-measures ANOVA for saccadic RT (a mean of 231 msec and a standard deviation of 33 msec across all conditions) during high TMS intensity. We predicted a main effect of TMS frequency or an interaction of TMS frequency with the other experimental factors. Consistent with our predictions, we found a main effect of TMS frequency, $F(1, 15) = 5.37$, $p = .035$, $\eta^2_p = .26$, and an interaction between TMS Frequency × TMS Site, $F(1, 15) = 5.50$, $p = .033$, $\eta^2_p = .27$. The interaction of TMS Frequency × TMS Site suggested that gamma and beta frequency TMS induced different effects when applied to IPS and sPCS. Therefore, we separately compared the effect of beta versus gamma frequency TMS in sPCS and IPS using post hoc tests, while controlling for multiple comparisons using the Tukey procedure. We found a significant difference between gamma and beta frequency TMS in sPCS, $t(15) = 3.29$, Tukey adjusted $p = .005$, $d = 0.82$ (Figure 2A), but no difference between gamma and beta frequency TMS in IPS, $t(15) = 0.76$, Tukey adjusted $p = .46$, $d = 0.19$. This effect was driven by a slowing of saccadic RTs after gamma frequency TMS to sPCS relative to control TMS, $t(15) = 3.42$, Tukey adjusted $p = .008$, $d = 0.86$ (Figure 2A), whereas beta frequency TMS to sPCS had no effect on saccadic RT, $t(15) = -0.48$, Tukey's adjusted $p = .87$, $d = 0.12$ (Figure 2A). The results from all conditions for saccadic RT are displayed in Figure 3A. Consistent with our hypothesis that gamma frequency oscillations would impact bottom–up attention, our results demonstrated that gamma frequency TMS to sPCS increased saccadic RT during both the feature and conjunction search tasks. The three-way (Task Condition × TMS Frequency × TMS Site) repeated-measures ANOVA for saccadic RT during low-intensity TMS did not reveal a significant main effect of TMS frequency, $F(1, 15) = 3.12$, $p = .098$, $\eta^2_p = .17$, nor an interaction between TMS frequency and TMS site, $F(1, 15) = 3.52$, $p = .080$, $\eta^2_p = .19$.

Given the lateralized receptive fields in sPCS and IPS, we predicted that gamma frequency TMS to the right

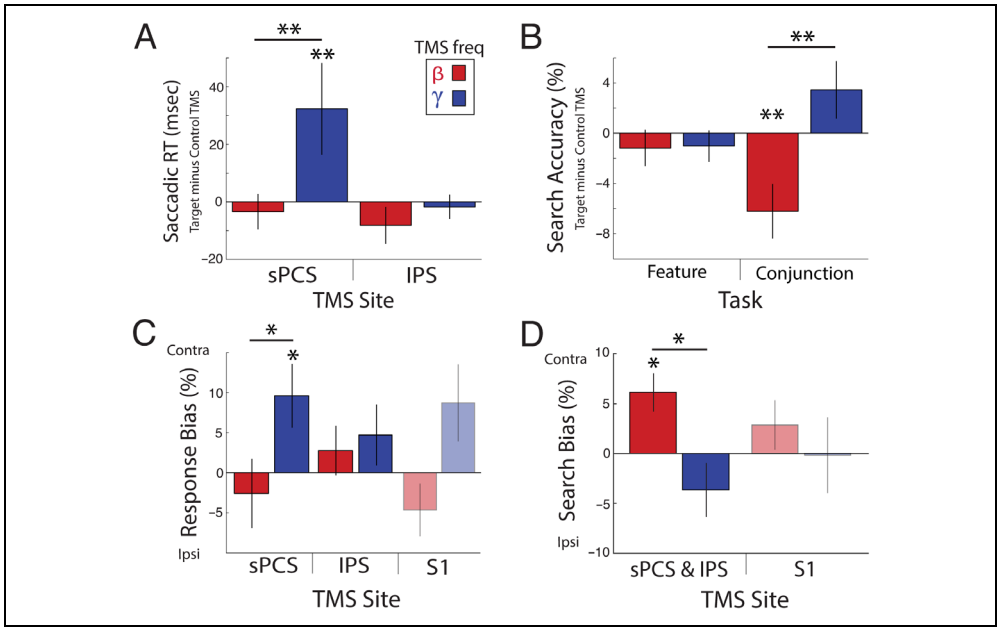

Figure 2. Frequency-specific high-intensity TMS effects on saccadic RT (A) and search accuracy (B). Analysis of conjunction search error trials for response bias (C) and search bias (D). Beta TMS is depicted in red; and gamma TMS, in blue. Error bars display the standard error to the mean. *Tukey's adjusted $p < .05$; **Tukey's adjusted $p < .01$. freq = frequency; Contra = contralateral; Ipsi = ipsilateral.

sPCS or IPS would cause a saccadic response bias toward the contralateral visual field. To test this hypothesis, we analyzed the direction of the first saccade for all error trials during the conjunction search task after high-intensity TMS. There were not enough errors in the feature search task to include Task as a factor in this analysis. A two-way repeated-measures ANOVA (TMS Frequency × TMS Site) during high-intensity TMS revealed a main effect of TMS frequency, $F(1, 15) = 5.69$, $p = .031$, $\eta^2_p = .28$ (Figure 2C). Consistent with our hypothesis, post hoc tests revealed a significant difference in response bias between gamma and beta TMS for sPCS, $t(15) = 2.56$, Tukey adjusted $p = .022$, $d = 0.64$, but not for IPS, $t(15) = 0.41$, Tukey adjusted $p = .69$, $d = 0.10$. Specifically, gamma TMS to sPCS resulted in a contralateral response bias, $t(15) = 2.51$, Tukey adjusted $p = .048$, $d = 0.63$, whereas there was no response bias after beta TMS, $t(15) = -0.68$, Tukey adjusted $p = .76$, $d = 0.17$. Neither beta nor gamma frequency TMS to the control S1 site caused a saccadic response bias. A two-way repeated-measures ANOVA (TMS Frequency × TMS Site) during high-intensity TMS for saccadic response bias did not reveal a significant main effect or interaction with TMS frequency. All conditions for response bias are displayed in Figure 3C.

Task Effects: Search Accuracy

We further tested how frequency-specific TMS would impact visual search accuracy. We performed a three-way (Task × TMS Frequency × TMS Site) repeated-measures ANOVA on search accuracy (a mean of 72% and a standard deviation of 8% across all conditions) during high-intensity TMS. This analysis revealed a significant main effect of TMS frequency, $F(1, 15) = 8.97$, $p = .0091$, $\eta^2_p = .37$, and a significant interaction between TMS frequency and Task, $F(1, 15) = 4.81$, $p = .044$, $\eta^2_p = .24$ (Figure 2B). The interaction of TMS Frequency × Task suggested that rhythmic TMS had different effects on search accuracy for the conjunction versus feature search task depending on the frequency of stimulation. Post hoc tests revealed a significant difference between beta and gamma frequency TMS for conjunction search, $t(15) = 3.77$, Tukey adjusted $p = .0018$, $d = 0.94$, but not feature search, $t(15) = 0.16$, Tukey adjusted $p = .88$, $d = 0.04$. Specifically, compared with control S1 TMS during the conjunction search task, only beta frequency TMS impaired search accuracy, $t(15) = -3.32$, Tukey adjusted $p = .0093$, $d = 0.83$, but not gamma frequency TMS, $t(15) = 1.72$, Tukey adjusted $p = .20$, $d = 0.43$. The results from all conditions for search accuracy are displayed in Figure 3B. A three-way (Task × TMS Frequency × TMS Site) repeated-measures ANOVA on search accuracy during low-intensity TMS did not reveal a significant main effect or interactions with TMS frequency.

Given the lateralized receptive fields in sPCS and IPS, beta frequency TMS could lead to a conjunction search bias toward the contralateral visual field. Thus, we predicted that beta frequency TMS would increase errors when the target was in the ipsilateral relative to the

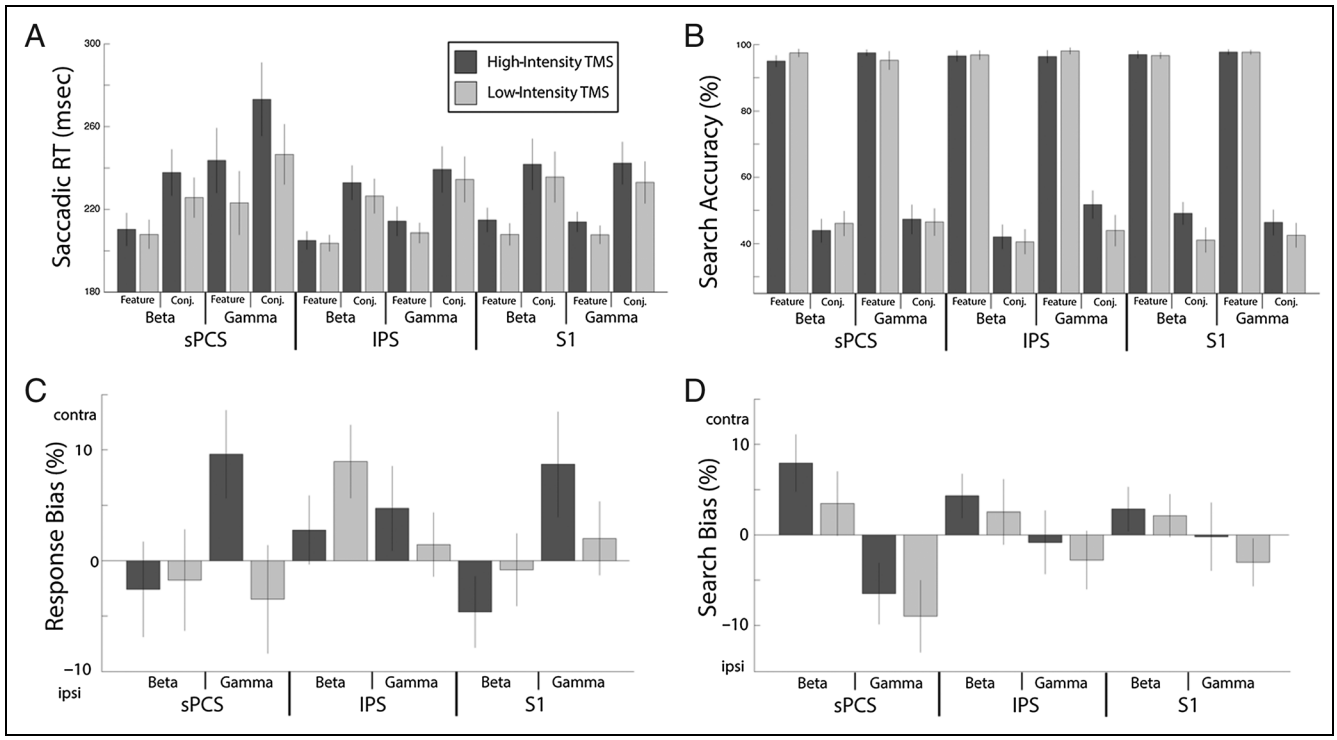

Figure 3. All behavioral conditions for (A) saccadic RT, (B) search accuracy, (C) response bias, and (D) search bias. High-intensity TMS is depicted in dark gray; and low intensity, in light gray. Error bars display the standard error to the mean. Conj. = conjunction.

contralateral visual field. To test this prediction, we performed a two-way repeated-measures ANOVA (TMS Frequency × TMS Site) on error trials in the conjunction search condition during high-intensity TMS. There were not enough error trials during feature search to perform the analysis. We found a main effect of TMS frequency, $F(1, 15) = 12.7$, $p = .0029$, $\eta^2_p = .46$ (Figure 2D). Consistent with our hypothesis, we found that there was a search bias toward the contralateral visual field after TMS to sPCS and IPS for beta frequency, $t(15) = 2.65$, Tukey adjusted $p = .036$, $d = 0.66$, but not gamma frequency, $t(15) = -1.59$, Tukey adjusted $p = .25$, $d = 0.40$. Neither beta nor gamma frequency TMS to the control S1 site caused a search bias. A two-way repeated-measures ANOVA (TMS Frequency × TMS Site) on error trials in the conjunction search condition during low-intensity TMS revealed a similar but weaker main effect of TMS frequency, $F(1, 15) = 5.73$, $p = .030$, $\eta^2_p = .28$. However, post hoc t tests were not significant. All conditions for search bias are displayed in Figure 3D.

DISCUSSION

Our results demonstrated that rhythmic TMS at specific frequencies can modulate specific cognitive processes. Moreover, these findings provide causal evidence supporting the proposal that top–down attention is mediated by beta frequency neuronal oscillations, whereas bottom–up attention is mediated by gamma frequency neuronal oscillations (Buschman & Miller, 2007).

Specifically, we found that gamma frequency TMS to sPCS slowed saccadic RTs during both feature and conjunction search conditions, both of which required bottom–up attention. Furthermore, we found that gamma frequency TMS to sPCS increased response bias to the contralateral visual field. Consistent with our findings, a previous study found that gamma, but not beta, frequency TMS to sPCS produced a bias toward reporting a low contrast stimulus in the contralateral visual field even if it was not present, perhaps because of a phantom bottom–up signal induced by gamma frequency TMS (Chanes et al., 2013). Direct projections from visual areas, such as V4, to sPCS (Schall, Morel, King, & Bullier, 1995) form a bottom–up pathway for stimulus-driven visual information, and this pathway exhibits increased interareal coherence in the gamma frequency during attention (Gregoriou et al., 2009). sPCS also has direct projections to the superior colliculus, and direct stimulation to sPCS in animals elicits saccadic eye movements (Robinson & Fuchs, 1969). Given this known circuitry, gamma frequency TMS to sPCS in our study may have disrupted gamma coherence between early visual regions and sPCS, which disrupted processing of salient visual stimuli, resulting in slower saccadic RTs. Slower saccadic RTs could reflect diminished transmission of bottom–up excitatory visual input from visual cortex to sPCS that is necessary to guide saccade generation in both tasks.

Electrophysiology studies using monkeys found that the analog to sPCS was the recipient of gamma-band oscillatory signals from IPS (Buschman & Miller, 2007). Although we did not record electrophysiology, gamma rhythmic TMS could have modulated the receptivity of sPCS to input timed to gamma frequency. Rhythmic TMS has been demonstrated to induce a phase reset in ongoing neuronal oscillations (Thut et al., 2011). If gamma frequency TMS reset the ongoing gamma phase, neuronal activity in sPCS could have become misaligned to incoming gamma frequency signals from IPS for bottom–up attention. Despite previous evidence of causal influence from IPS to sPCS during bottom–up attention, the lack of a behavioral effect from gamma frequency TMS to IPS suggests either that task-related gamma oscillations in IPS was not significantly modulated or that the reception of gamma frequency activity in sPCS was more critical to bottom–up attention.

Alternatively, gamma frequency TMS to sPCS may have impacted local gamma frequency neuronal oscillations and induced a signal that mimicked bottom–up signals from visual cortex. These induced local gamma frequency neuronal oscillations could have driven bottom–up attention toward the contralateral visual field, resulting in a response bias toward the contralateral visual field. The communication through coherence hypothesis suggests that gamma frequency oscillations modulate excitation–inhibition balance for bottom–up attention selection (Fries, 2015). In this model, excitatory activity within a neural circuit triggered by sensory input can be dampened by local inhibitory interneurons, resulting in an inactivation period that lasts roughly the duration of a gamma cycle (Börgers & Kopell, 2007). As the inactivation period expires, the neural circuit becomes ready for a new volley of excitatory input. Therefore, a neural circuit can be more sensitive to excitatory input timed to the gamma frequency range (Börgers & Kopell, 2007). In our study, gamma frequency TMS timed to the resonant frequency of excitatory bottom–up information could have driven the excitatory signaling pathway that is usually triggered in response to contralateral visual stimuli transmitted from the visual cortex. In this way, gamma frequency TMS could have driven bottom–up attention by mimicking the activity of a salient stimuli in the contralateral visual field, leading to a saccade.

A possible alternative account for our gamma frequency TMS effects is that our results could be explained by its impact on saccade generation mechanisms rather than bottom–up attention. Previous studies have shown beta frequency stimulation to be antikinetic whereas gamma frequency is prokinetic (Joundi, Jenkinson, Brittain, Aziz, & Brown, 2012); thus, on the basis of these results, one could have made the prediction that gamma frequency TMS would speed up saccade latencies, not slow them down. In addition, on the basis of this prior

work, TMS in both frequencies should have affected eye movements, not just gamma TMS. Furthermore, in a previous behavioral study (Heeman, Van der Stigchel, & Theeuwes, 2017) where participants were encouraged to make short latency saccades in the presence of distractors, it was observed that, with shorter saccade RTs, there was increased response bias. This finding suggests that, if gamma TMS slowed saccadic RTs, we should have observed less response bias, but we observed more response bias. This suggests that gamma TMS likely has an effect on task-related processes in addition to saccade generation. Finally, another study that applied gamma frequency TMS to sPCS found an increased bias toward reporting a low contrast stimulus in the contralateral field, which is consistent with our findings (Chanes et al., 2013). Considering these findings, we believe that gamma frequency TMS more likely impacted bottom–up attentional processes rather than saccade metrics alone.

Consistent with previous neurophysiology studies that showed beta coherence between sPCS and IPS during top–down attention (Buschman & Miller, 2007), we found that beta, but not gamma, frequency TMS disrupted search accuracy when applied to both sPCS and IPS during the conjunction search condition. Beta-band oscillations are found during a variety of tasks that require top–down attention (Engel & Fries, 2010). For example, during the delay period of a delayed matched-to-sample task performed by monkeys, prefrontal cortex ventral to the principal sulcus and FEFs exhibit an increase in beta oscillatory bursts that track the maintenance of a stimulus representation (Lundqvist et al., 2016). In addition, when making categorical judgments about presented stimuli, coherent beta frequency oscillations between frontal and parietal cortex increase stimulus-driven gamma frequency oscillations in regions that represent task-relevant information (Antzoulatos & Miller, 2016).

A previous monkey electrophysiology study found that beta-band oscillatory signals transmitted from sPCS to IPS increased with more top–down attention (Buschman & Miller, 2007). Because search accuracy was impaired after beta frequency TMS to both sPCS and IPS, there are several possible neural mechanisms to explain this finding. For example, beta TMS may have altered the generation of top–down beta frequency signals emanating directly from sPCS, altered the receptivity of beta frequency signals in IPS from sPCS, or impacted overall beta frequency signal coherence between sPCS and IPS.

We further found that, when beta frequency TMS was applied to sPCS and IPS during the conjunction search condition, participants' errors were concentrated to trials in which the target was in the ipsilateral visual field. Beta frequency oscillations during a similar conjunction search task have been found to track the serial shift of a single spotlight of attention through each item within a probe array of four different stimuli (Buschman & Miller, 2009). Thus, our findings could indicate that beta frequency TMS shifted serial search toward the contralateral visual field through exogenously entrained beta oscillations, at the expense of visual search in the ipsilateral side. Therefore, despite the decrease in overall search accuracy, beta frequency rhythmic TMS could have increased top–down attention signals to the contralateral visual field. Our results are also consistent with a previously mentioned study that found that only beta, not gamma, frequency TMS to sPCS increased contralateral perceptual sensitivity (Chanes et al., 2013).

Beta oscillations between frontal and parietal regions modulate gamma oscillations to increase tuning (Stanley et al., 2016), bias gamma activity toward processing relevant categories (Antzoulatos & Miller, 2014), and boost gamma activity corresponding to active stimulus processing (Richter, Thompson, Bosman, & Fries, 2017). Layer-specific recordings demonstrate that beta oscillations are expressed more strongly in the deep layers, whereas gamma oscillations are stronger in the superficial layers (Bastos, Loonis, Kornblith, Lundqvist, & Miller, 2018) and that beta oscillations in deep layers act to modulate the superficial layers (Bastos et al., 2018). Given that our results showed that rhythmic TMS to a single cortical region in beta versus gamma frequency has different effects on behavior, rhythmic TMS could have causally modulated specific layers of cortex and their associated top–down and bottom–up signaling pathways.

In our study, gamma TMS began at 120 msec after probe and beta TMS began at 30 msec after probe, and both trains of rhythmic TMS ended at 180 msec after probe. The specific timing was chosen to maximize the effects of rhythmic TMS during the window of time just before a saccadic response in which task-relevant beta and gamma oscillations were found (Buschman & Miller, 2007). However, differences in the time course of activation for sPCS and IPS and the different timing of beta and gamma frequency TMS relative to the probe could present a potential confound. For example, we found decreased saccade accuracy after beta frequency TMS to IPS but no effect of gamma frequency TMS to IPS. If IPS processes information within 120 msec after the probe, then IPS would not be affected by gamma frequency TMS because it was delivered after that period. Thus, the effect of beta frequency TMS on IPS may not be because of its effect on beta frequency neuronal oscillations but instead because of the time it was given. However, it is unlikely that IPS was only active in the first 120 msec after presentation of the probe, as a robust increase in parietal cortex neuronal firing to salient visual stimuli has been repeatedly observed from the onset of the probe until the saccadic response (Buschman & Miller 2007; Gottlieb, Kusunoki, & Goldberg, 1998).

Although our study focused on gamma and beta oscillations, other neuronal oscillations may be relevant to visual search. Gamma frequency neuronal oscillations have

been implicated in a generalized theta–gamma neural coding scheme for perception (Lisman & Jensen, 2013). In the theta–gamma neural code, high-frequency gamma coherence conveys the specific bottom–up information in perception, whereas the theta frequency oscillation serves as a means of binding representations (Clouter, Shapiro, & Hanslmayr, 2017; Heusser, Poeppel, Ezzyat, & Davachi, 2016; Klimesch, Doppelmayr, Russegger, & Pachinger, 1996) or acts as a carrier frequency for long-distance coordination of bottom–up information processing (Solomon et al., 2017). A previous theta frequency TMS study found that stimulation boosted perceptual sensitivity to a global gestalt that required increased perceptual binding (Romei et al., 2011). Although our task does not require gestalt perception, the conjunctive feature search condition required the binding of color and orientation that may be processed by theta–gamma coding. In addition, gamma frequency TMS could have impacted theta oscillations given the theta–gamma coding scheme. Finally, theta frequency has been implicated in the rhythmic sampling of visual information (Fiebelkorn, Pinsk, & Kastner, 2018; Helfrich et al., 2018; Busch & VanRullen, 2010); however, these studies often rely on stimuli to be presented over a longer epoch on the order of seconds.

Alpha frequency neuronal oscillations have also been shown to play a role in top–down visual processing and visual attention in particular (Wang, Rajagovindan, Han, & Ding, 2016). Alpha frequency oscillations have an inverse relationship to cortical processing, where increased alpha activity corresponds to a decrease in bottom–up information processing (Klimesch, Sauseng, & Hanslmayr, 2007). By increasing the number of distractors, alpha activity can be driven in the regions that process those distractors (Sauseng et al., 2009). Alpha and beta oscillations are dissociable (Strauß, Kotz, Scharinger, & Obleser, 2014), and whereas alpha oscillations are inhibitory, beta oscillations have been shown to boost bottom–up cortical activity (Richter et al., 2017). Using frequency-specific alternating current stimulation, beta, but not alpha, frequency stimulation has been shown to decrease phosphene threshold in occipital cortex, providing further causal evidence that beta oscillations boost visual processing (Kanai, Chaieb, Antal, Walsh, & Paulus, 2008). In contrast, alpha oscillations are specifically recruited by visual attention to suppress bottom–up information processing when attention is cued to a spatial location before stimulus presentation (Liu, Bengson, Huang, Mangun, & Ding, 2016; Wallis, Stokes, Cousijn, Woolrich, & Nobre, 2015; Kelly, Lalor, Reilly, & Foxe, 2006). Multiple studies have found that alpha frequency TMS ipsilateral to the focus of visual attention improves target detection (Romei et al., 2010; Sauseng et al., 2009). However, in the visual search task used here, the target location is unpredictable and randomized and thus does not engage prestimulus visual attention, which has been linked to alpha oscillations. Thus, it is unlikely that our task engages retinotopic alpha oscillations that have been reported in previous studies with visual attention.

Collecting EEG during the delivery of rhythmic TMS has proven useful in verifying entrainment of neuronal oscillations in the targeted frequency band. These studies have found that repeated TMS pulses focus oscillatory power at the targeted frequency (theta: Albouy et al., 2017; beta: Hanslmayr et al., 2014; alpha: Thut et al., 2011). Although we did not collect TMS-EEG, one previous study verified entrainment of beta frequency oscillations that persisted after delivery of beta frequency rhythmic TMS (Hanslmayr et al., 2014). However, EEG measurements of beta frequency oscillations were not possible during beta frequency TMS because of the corruption of the EEG signal with each TMS pulse (Hanslmayr et al., 2014). Given that, in our study, a response is made immediately after completion of TMS, it is likely that evidence of entrainment would be corrupted by the motor response. To investigate entrainment during the delivery of high-frequency stimulation (greater than 10 Hz), electrical activity would need to be recorded without the low-pass filter of the skull, which is possible either in electrocorticography in humans or in animal models. EEG is suboptimal for measuring gamma frequency oscillations because of the low-pass filter of the skull; thus, entrainment of gamma frequency oscillations from rhythmic TMS has not been reported. Despite these limitations inherent to rhythmic TMS, our study provides causal evidence for the mechanistic role of beta and gamma oscillations in cognition and suggests that the interpulse interval of TMS trains is critical to its behavioral impact.

Acknowledgments

This work was supported by National Institues of Health grants MH11173 and MH103842 and National Science Foundation grant DGE 1106400.

Reprint requests should be sent to Justin Riddle, University of California, Berkeley, 10 Giannini Hall, Berkeley, CA 94720, or via e-mail: riddler@berkeley.edu.

REFERENCES

Albouy, P., Weiss, A., Baillet, S., & Zatorre, R. J. (2017). Selective entrainment of theta oscillations in the dorsal stream causally enhances auditory working memory performance. *Neuron*, *94*, 193.e5–206.e5.

Antzoulatos, E. G., & Miller, E. K. (2014). Increases in functional connectivity between prefrontal cortex and striatum during category learning. *Neuron*, *83*, 216–225.

Antzoulatos, E. G., & Miller, E. K. (2016). Synchronous beta rhythms of frontoparietal networks support only behaviorally relevant representations. *eLife*, *5*, 1–22.

Bastos, A. M., Loonis, R., Kornblith, S., Lundqvist, M., & Miller, E. K. (2018). Laminar recordings in frontal cortex suggest distinct layers for maintenance and control of working memory. *Proceedings of the National Academy of Sciences, U.S.A.*, *115*, 1117–1122.

Bastos, A. M., Vezoli, J., Bosman, C. A., Schoffelen, J. M., Oostenveld, R., Dowdall, J. R., et al. (2015). Visual areas exert

feedforward and feedback influences through distinct frequency channels. *Neuron*, *85*, 390–401.
Börgers, C., & Kopell, N. (2007). Gamma oscillations and stimulus selection. *Neural Computation*, *20*, 383–414.
Busch, N., & VanRullen, R. (2010). Spontaneous EEG oscillations reveal periodic sampling of visual attention. *Proceedings of the National Academy of Sciences, U.S.A.*, *107*, 10648–16053.
Buschman, T. J., & Miller, E. K. (2007). Top–down versus bottom–up control of attention in the prefrontal and posterior parietal cortices. *Science*, *315*, 1860–1862.
Buschman, T. J., & Miller, E. K. (2009). Serial, covert shifts of attention during visual search are reflected by the frontal eye fields and correlated with population oscillations. *Neuron*, *63*, 386–396.
Buzsáki, G. (2006). *Rhythms of the brain*. New York: Oxford University Press.
Cameron, I. G. M., Riddle, J. M., & D'Esposito, M. (2015). Dissociable roles of dorsolateral prefrontal cortex and frontal eye fields during saccadic eye movements. *Frontiers in Human Neuroscience*, *9*, 613.
Canolty, R. T., & Knight, R. T. (2010). The functional role of cross-frequency coupling. *Trends in Cognitive Sciences*, *14*, 506–515.
Chanes, L., Quentin, R., Tallon-Baudry, C., & Valero-Cabré, A. (2013). Causal frequency-specific contributions of frontal spatiotemporal patterns induced by non-invasive neurostimulation to human visual performance. *Journal of Neuroscience*, *33*, 5000–5005.
Clouter, A., Shapiro, K. L., & Hanslmayr, S. (2017). Theta phase synchronization is the glue that binds human associative memory. *Current Biology*, *27*, 3143.e6–3148.e6.
Corbetta, M., & Shulman, G. L. (2002). Control of goal-directed and stimulus-driven attention in the brain. *Nature Reviews Neuroscience*, *3*, 201–215.
Cox, R. W. (1996). AFNI: Software for analysis and visualization of functional resonance neuroimages. *Computers and Biomedical Research*, *29*, 162–173.
Dale, A. (1999). Optimal experimental design for event-related fMRI. *Human Brain Mapping*, *8*, 109–114.
Donner, T. H., Kettermann, A., Diesch, E., Ostendorf, F., Villringer, A., & Brandt, S. A. (2002). Visual feature and conjunction searches of equal difficulty engage only partially overlapping frontoparietal networks. *Neuroimage*, *15*, 16–25.
Engel, A. K., & Fries, P. (2010). Beta-band oscillations—Signaling the status quo? *Current Opinion in Neurobiology*, *20*, 156–165.
Fiebelkorn, I. C., Pinsk, M. A., & Kastner, S. (2018). A dynamic interplay within the frontoparietal network underlies rhythmic spatial attention. *Neuron*, *99*, 842.e8–853.e8.
Fries, P. (2015). Rhythms for cognition: Communication through coherence. *Neuron*, *88*, 220–235.
Fröhlich, F., & McCormick, D. A. (2010). Endogenous electric fields may guide neocortical network activity. *Neuron*, *67*, 129–143.
Gottlieb, J. P., Kusunoki, M., & Goldberg, M. E. (1998). The representation of visual salience in monkey parietal cortex. *Nature*, *391*, 481–484.
Grefkes, C., & Fink, G. R. (2005). The functional organization of the intraparietal sulcus in humans and monkeys. *Journal of Anatomy*, *207*, 3–17.
Gregoriou, G. G., Gotts, S. J., Zhou, H., & Desimone, R. (2009). High-frequency, long-range coupling between prefrontal and visual cortex during attention. *Science*, *324*, 1207–1210.
Hanslmayr, S., Matuschek, J., & Fellner, M. C. (2014). Entrainment of prefrontal beta oscillations induces an endogenous echo and impairs memory formation. *Current Biology*, *24*, 904–909.
Heeman, J., Van der Stigchel, S., & Theeuwes, J. (2017). The influence of distractors on express saccades. *Journal of Vision*, *17*, 35.
Helfrich, R. F., Fiebelkorn, I. C., Szczepanski, S. M., Lin, J. J., Parvizi, J., Knight, R. T., et al. (2018). Neural mechanisms of sustained attention are rhythmic. *Neuron*, *99*, 854–865.
Heusser, A. C., Poeppel, D., Ezzyat, Y., & Davachi, L. (2016). Episodic sequence memory is supported by a theta-gamma phase code. *Nature Neuroscience*, *19*, 1374–1380.
Joundi, R. A., Jenkinson, N., Brittain, J. S., Aziz, T. Z., & Brown, P. (2012). Driving oscillatory activity in the human cortex enhances motor performance. *Current Biology*, *22*, 403–407.
Kanai, R., Chaieb, L., Antal, A., Walsh, V., & Paulus, W. (2008). Frequency-dependent electrical stimulation of the visual cortex. *Current Biology*, *18*, 1839–1843.
Kelly, S. P., Lalor, E. C., Reilly, R. B., & Foxe, J. J. (2006). Increases in alpha oscillatory power reflect an active retinotopic mechanism for distracter suppression during sustained visuospatial attention. *Journal of Neurophysiology*, *95*, 3844–3851.
Klimesch, W., Doppelmayr, M., Russegger, H., & Pachinger, T. (1996). Theta band power in the human scalp EEG and the encoding of new information. *NeuroReport*, *7*, 1235–1240.
Klimesch, W., Sauseng, P., & Hanslmayr, S. (2007). EEG alpha oscillations: The inhibition–timing hypothesis. *Brain Research Reviews*, *53*, 63–88.
Kornblith, S., Buschman, T. J., & Miller, E. K. (2016). Stimulus load and oscillatory activity in higher cortex. *Cerebral Cortex*, *26*, 3772–3784.
Lisman, J. E., & Jensen, O. (2013). The theta-gamma neural code. *Neuron Perspective*, *77*, 1002–1016.
Liu, Y., Bengson, J., Huang, H., Mangun, G. R., & Ding, M. (2016). Top–down modulation of neural activity in anticipatory visual attention: Control mechanisms revealed by simultaneous EEG-fMRI. *Cerebral Cortex*, *26*, 517–529.
Lundqvist, M., Rose, J., Herman, P., Brincat, S. L., Buschman, T. J., & Miller, E. K. (2016). Gamma and beta bursts underlie working memory. *Neuron*, *90*, 152–164.
Marshall, T. R., O'Shea, J., Jensen, O., & Bergmann, T. O. (2015). Frontal eye fields control attentional modulation of alpha and gamma oscillations in contralateral occipitoparietal cortex. *Journal of Neuroscience*, *35*, 1638–1647.
Michalareas, G., Vezoli, J., van Pelt, S., Schoffelen, J. M., Kennedy, H., & Fries, P. (2016). Alpha-beta and gamma rhythms subserve feedback and feedforward influences among human visual cortical areas. *Neuron*, *89*, 384–397.
Muggleton, N. G., Juan, C. H., Cowey, A., & Walsh, V. (2003). Human frontal eye fields and visual search. *Journal of Neurophysiology*, *89*, 3340–3343.
Nakayama, K., & Silverman, G. H. (1986). Serial and parallel processing of visual feature conjunctions. *Nature*, *320*, 264–265.
O'Shea, J., Johansen-Berg, H., Trief, D., Göbel, S., & Rushworth, M. F. (2007). Functionally specific reorganization in human premotor cortex. *Neuron*, *54*, 479–490.
Quentin, R., Elkin Frankston, S., Vernet, M., Toba, M. N., Bartolomeo, P., Chanes, L., et al. (2016). Visual contrast sensitivity improvement by right frontal high-beta activity is mediated by contrast gain mechanisms and influenced by fronto-parietal white matter microstructure. *Cerebral Cortex*, *26*, 2381–2390.
Reuter-Lorenz, P. A., Hughes, H. C., & Fendrich, R. (1991). The reduction of saccadic latency by prior offset of the fixation point: An analysis of the gap effect. *Perception Psychophysics*, *49*, 167–175.
Richter, C. G., Thompson, W. H., Bosman, C. A., & Fries, P. (2017). Top–down beta enhances bottom–up gamma. *Journal of Neuroscience*, *37*, 6698–6711.

Robinson, D. A., & Fuchs, A. F. (1969). Eye movements evoked by stimulation of frontal eye fields. *Journal of Neurophysiology*, *32*, 637–648.
Romei, V., Driver, J., Schyns, P. G., & Thut, G. (2011). Rhythmic TMS over parietal cortex links distinct brain frequencies to global versus local visual processing. *Current Biology*, *21*, 334–337.
Romei, V., Gross, J., & Thut, G. (2010). On the role of prestimulus alpha rhythms over occipito-parietal areas in visual input regulation: Correlation or causation? *Journal of Neuroscience*, *30*, 8692–8697.
Sauseng, P., Klimesch, W., Heise, K. F., Gruber, W. R., Holz, E., Karim, A. A., et al. (2009). Brain oscillatory substrates of visual short-term memory capacity. *Current Biology*, *19*, 1846–1852.
Schall, J. D., Morel, A., King, D., & Bullier, J. (1995). Topography of visual cortex connections with frontal eye field in Macaque: Convergence and segregation of processing streams. *Journal of Neuroscience*, *15*, 4464–4487.
Shulman, G. L., McAvoy, M. P., Cowan, M. C., Astafiev, S. V., Tansy, A. P., d'Avossa, G., et al. (2003). Quantitative analysis of attention and detection signals during visual search. *Journal of Neurophysiology*, *90*, 3384–3397.
Siegel, M., Donner, T. H., & Engel, A. K. (2012). Spectral fingerprints of large-scale neuronal interactions. *Nature Reviews Neuroscience*, *13*, 121–134.
Silver, M. A., & Kastner, S. (2009). Topographic maps in human frontal and parietal cortex. *Trends in Cognitive Sciences*, *13*, 488–495.
Solomon, E. A., Kragel, J. E., Sperling, M. R., Sharan, A., Worrell, G., Kucewicz, M., et al. (2017). Widespread theta synchrony and high-frequency desynchronization underlies enhanced cognition. *Nature Communications*, *8*, 1704.
Stanley, D. A., Roy, J. E., Aoi, M. C., Kopell, N. J., & Miller, E. K. (2016). Low-beta oscillations turn up the gain during category judgements. *Cerebral Cortex*, *28*, 116–130.
Stokes, M. G., Chambers, C. D., Gould, I. C., Henderson, T. R., Janko, N. E., Allen, N. B., et al. (2005). Simple metric for scaling motor threshold based on scalp-cortex distance: Application to studies using transcranial magnetic stimulation. *Journal of Neurophysiology*, *94*, 4520–4527.
Stoll, F. M., Wilson, C. R. E., Faraut, M. C. M., Vezoli, J., Knoblauch, K., & Procyk, E. (2016). The effects of cognitive control and time on frontal beta oscillations. *Cerebral Cortex*, *26*, 1715–1732.
Strauß, A., Kotz, S. A., Scharinger, M., & Obleser, J. (2014). Alpha and theta brain oscillations index dissociable processes in spoken word recognition. *Neuroimage*, *97*, 387–395.
Thut, G., Veniero, D., Romei, V., Miniussi, C., Schyns, P., & Gross, J. (2011). Rhythmic TMS causes local entrainment of natural oscillatory signatures. *Current Biology*, *21*, 1176–1185.
Treisman, A. M., & Gelade, G. (1980). A feature-integration theory of attention. *Cognitive Psychology*, *12*, 97–136.
Vernet, M., Quentin, R., Chanes, L., Mitsumasu, A., & Valero-Cabré, A. (2014). Frontal eye field, where art thou? Anatomy, function, and non-invasive manipulation of frontal regions involved in eye movements and associated cognitive operations. *Frontiers in Integrative Neuroscience*, *8*, 66.
Wagner, T., Rushmore, J., Eden, U., & Valero-Cabré, A. (2009). Biophysical foundations underlying TMS: Setting the stage for an effective use of neurostimulation in the cognitive neurosciences. *Cortex*, *45*, 1025–1034.
Wallis, G., Stokes, M., Cousijn, H., Woolrich, M., & Nobre, A. C. (2015). Frontoparietal and cingulo-opercular networks play dissociable roles in control of working memory. *Journal of Cognitive Neuroscience*, *27*, 2019–2034.
Wang, C., Rajagovindan, R., Han, S. M., & Ding, M. (2016). Top–down control of visual alpha oscillations: Sources of control signals and their mechanisms of action. *Frontiers in Human Neuroscience*, *10*, 15.